JOURNAL OF MATERIALS SCIENCE 21 (1986) 3703–3709

Stress-corrosion cracking and its propagation in aligned short-fibre composites

PAU-LO HSU*, SHI-SHEN YAU, TSU-WEI CHOU
Center for Composite Materials and Department of Mechanical and Aerospace Engineering, University of Delaware, Newark, Delaware 19716, USA

Stress-corrosion tests are conducted on aligned short-fibre composites to assess their performance in both air and 1 N H_2SO_4 environments. The materials used are 3 mm E-glass, AS4 carbon, and their hybrid fibre reinforced epoxy composites. Several crack propagation models are developed to describe different cracking behaviour; the observed composite fracture modes verify these proposed models. Pre-immersion has significant effects on K_I–t_f and crack arrest of hybrid composites. A comparison of theoretical and experimental K_I–t_f curves indicates good agreement of time to failure. The present research has quantified the susceptibility of these composites to environmental attack.

1. Introduction

Short-fibre composites are gaining wide applications in the chemical and automotive industries because of their improved performance. They offer the advantage of design flexibility and energy saving for high-rate productions. To date, short-fibre composites have been used mainly in secondary or non-weight bearing components. However, with the alignment of short fibres, there is the opportunity of enhancing the mechanical performance as well as the reliability of short-fibre composites; now they can be utilized as major load carrying members.

Highly aligned short-fibre composites have been produced successfully by the centrifuge [1] and vacuum [2] processes using a suspension medium containing the chopped fibres. The aligned short-fibre prepregs can minimize the longitudinal displacement or transverse splitting (which often occurs in continuous fibre prepregs) of the sheets during lay-up or moulding processes. Thus the main advantage of these materials is their capacity to form complex shapes. Since aligned short-fibre composites have the potential to be adopted in aerospace and aeronautic applications, their performance under aggressive environments is very important to the designers. Therefore, the study of composite degradation and crack resistance under stress–corrosion conditions is imperative.

The corrosion effects on both E-glass filaments and bundles were studied by Hsu and Chou [3]. They concluded that the pre-immersion process in 1 N H_2SO_4 resulted in the degradation of E-glass filament strength. The Weibull scale parameter was affected significantly, whereas the Weibull shape parameter was scarcely affected. In composite materials, the presence of a matrix, which provides protection to the reinforcing fibres against environmental attack, also adds to the complexity of the problem. Furthermore, the behaviour of composites under stress-corrosion is very different from that in the unstressed state. The stress-corrosion effects cannot be predicted by considering the mechanical and chemical effects separately. In fact, cracks produced by stress will propagate more rapidly under corrosion conditions. The present research aims for a better understanding of crack propagation modes and service life of aligned short-fibre composites under stress-corrosion conditions.

2. Experimental procedure

The materials used were aligned short-fibre composite mats (prepregs) fabricated by PERME (Propellants, Explosives and Rocket Motor Establishment), UK, using the centrifuge method. The reinforcements were 3 mm lengths of E-glass, AS4 carbon and a glass–carbon hybrid; the matrix was the Ciba–Geigy Fiberdux 914 epoxy resin. The diameter of glass fibre was about 10 μm, and that of carbon 7 μm. Table I lists the specifications of these composites. Composite laminates were laid up in a $(0°/90°/90°/0°)_3$ sequence, and cured at 120° C for 60 min and at 175° C for 100 min with a 3° C min^{-1} heating rate under 586 kPa pressure. Manders and Chou [4] examined the root mean square of fibre misorientation and reported the angles to be 6.8° in the plane of laminate and 2.4° perpendicular to that plane.

The composites were cut and fabricated into compact tension (CT) specimens per ASTM E399-83, the specimen size W being 50.8 mm. Since the average thickness of specimen was less than 2.5 mm, a plexiglass guide was used to prevent twisting of the

TABLE I Specifications of aligned short fibre composites

Fibre material	V_f (%)	Density (g cm^{-3})	Thickness (mm)
Glass	48.0	1.81	2.36
Carbon	48.1	1.42	2.77
Glass–carbon	47.0*	1.70	1.85

*Volume ratio of glass : carbon = 80 : 20.

*Present address: Mechanical Engineering Department, University of Wisconsin, Madison, Wisconsin 53706, USA.

0022–2461/86 $03.00 + .12

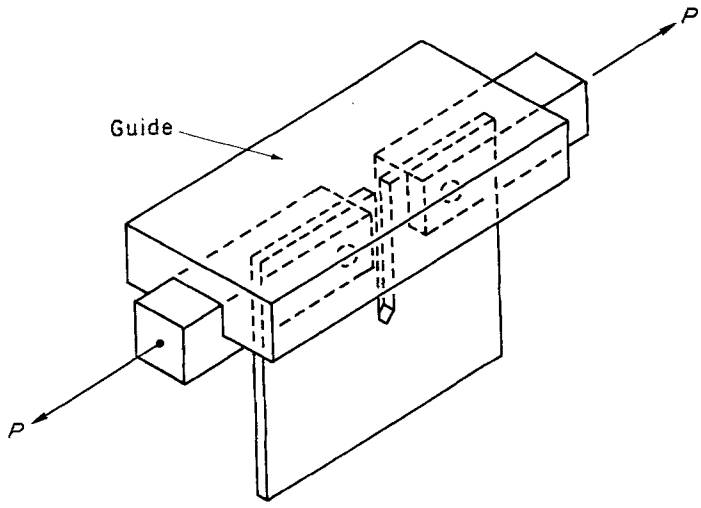

Figure 1 Schematic illustration of guide fixtures.

specimen (Fig. 1). Consequently, the crack propagated along the initial direction and the damage zone at the crack tip was minimized. The applicability of linear elastic fracture mechanics (LEFM) was also examined. The specimens were tested in air and 1 N H_2SO_4 environments, and load was applied using dead weights. The crack tip was monitored with a 60 × optical microscope; crack extension as small as 0.01 mm could be measured. Precracking of stress-corrosion specimens was conducted in the environmental chamber under full test conditions (1 N H_2SO_4), resulting in a sharp crack tip for subsequent stress-corrosion cracking experiments. The machined notch plus the precrack length gave a normalized crack length (a/W) of 0.33 for glass and hybrid specimens, and 0.5 for carbon specimens.

3. Results

Fig. 2 shows the $a-t$ (crack length against loading time) curve of glass composites tested in air. The crack propagation rate, which is represented by the slope of the curve, increases and decreases several times during the cracking process. Fig. 3 shows the $a-t$ curves for glass composites tested in 1 N H_2SO_4. Curves A and C illustrate the $a-t$ behaviour (without pre-immersion) for K_{Ii} (initial stress intensity factor) of 4.62 and 5.45 MPa $m^{1/2}$, respectively. Curve B is obtained from K_{Ii} of 4.13 MPa $m^{1/2}$ with 960 h (40 days) pre-immersion. Fig. 4 depicts the relationship between crack propagation rate and stress intensity factor for the above three cases. The crack propagation rate varies linearly with the stress intensity factor on the log scale; this is an indication that LEFM is obeyed.

In the case of carbon composites, the crack propagation behaviour is very irregular, and a meaningful $a-t$ curve cannot be obtained. Catastrophic failure of specimens occurs at various crack lengths in both air and acid environments. For glass–carbon hybrid composites, cracking behaviour observed in air (Fig. 5) is similar to that of glass composites. There are sudden changes in crack propagation rate in the fracture process, but the failure of

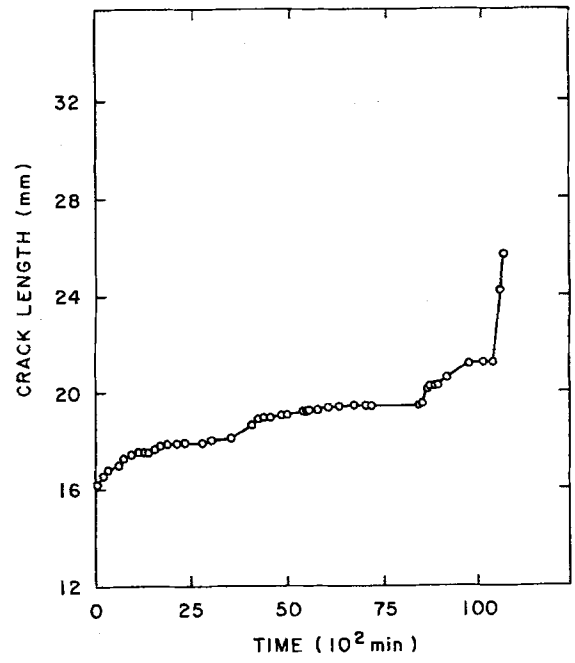

Figure 2 Crack growth curve of short-glass composites in air.

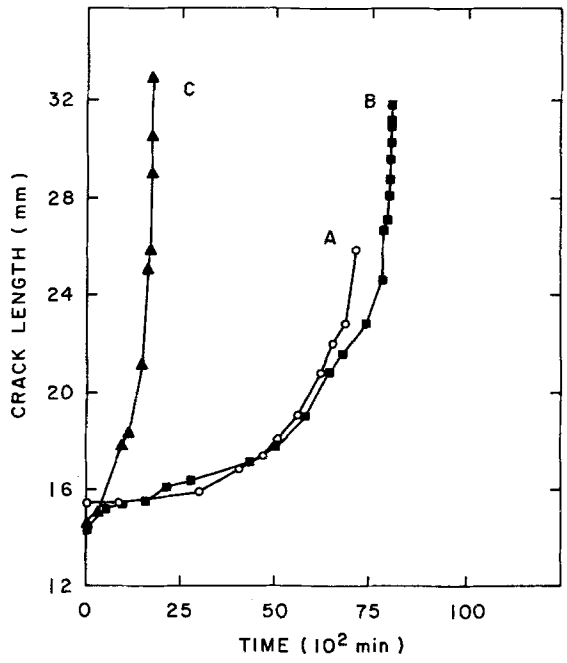

Figure 3 Crack growth curves of short-glass composites in 1 N H_2SO_4. Curve A, without pre-immersion, K_{Ii} = 4.62 MPa $m^{1/2}$; Curve B, with pre-immersion, K_{Ii} = 4.13 MPa $m^{1/2}$; Curve C, without pre-immersion, K_{Ii} = 5.45 MPa $m^{1/2}$.

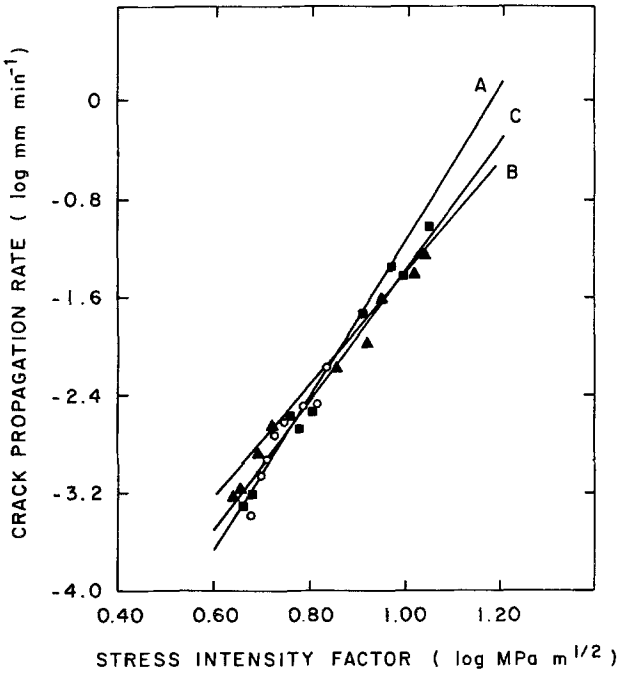

Figure 4 Crack propagation rate curves of short-glass composites in 1 N H_2SO_4. Curve A, without pre-immersion, K_{Ii} = 4.62 MPa m$^{1/2}$; Curve B, without pre-immersion, K_{Ii} = 5.45 MPa m$^{1/2}$; Curve C, with pre-immersion, K_{Ii} = 4.13 MPa m$^{1/2}$.

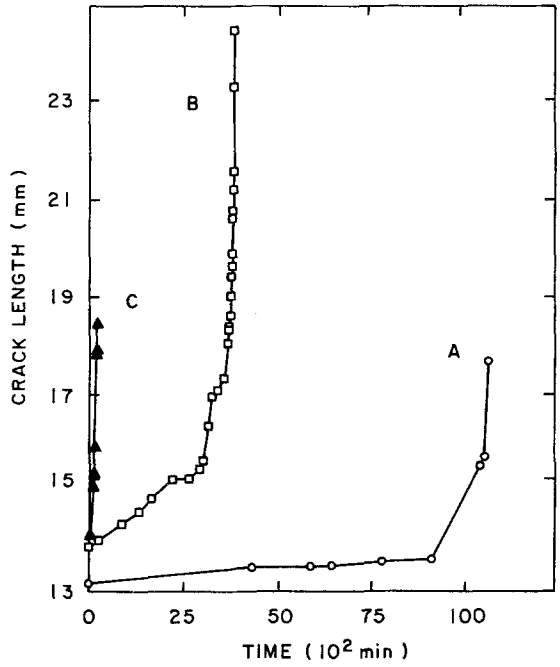

Figure 6 Crack growth curves of short-hybrid composites in 1 N H_2SO_4. Curve A, without pre-immersion, K_{Ii} = 6.59 MPa m$^{1/2}$; Curve B, without pre-immersion, K_{Ii} = 7.41 MPa m$^{1/2}$; Curve C, with pre-immersion, K_{Ii} = 7.16 MPa m$^{1/2}$.

specimens does not occur for an indefinite period. The results of the hybrid composites tested in acid without pre-immersion are shown in curves A and B of Fig. 6; there are also sudden changes in crack propagation rate. Curve C of Fig. 6 is for the case of a specimen with pre-immersion in acid for 60 days; there is no sudden change in crack propagation rate. Fig. 7 shows the failed hybrid specimen tested in acid, with and without pre-immersion. The pre-immersed specimen shows longer fibre bundle pull-out on the fracture surfaces.

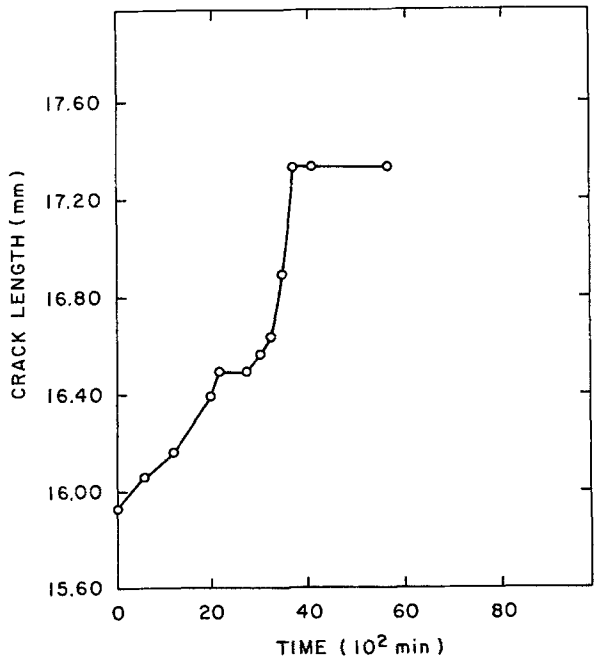

Figure 5 Crack growth curve of short-hybrid composites in air.

4. Discussions

4.1. Crack arrest effects

If crack propagation in composites obeys the LEFM prediction, a typical crack extension against time relationship should follow curve A in Fig. 8. The crack propagation rate can then be expressed as:

$$V = da/dt = CK_I^n \quad (1)$$

where V is the crack propagation rate, and n and C are material constants. However, crack tip blunting can take place due to the complicated failure mechanisms in composites such as debonding, as well as fibre pull-out and bridging. This tends to cause crack arrests; thus, two other types of a–t curves (B and C in Fig. 8) may appear. Both curves B and C display a slower crack extension rate than that of curve A. The change of crack propagation rate in curve B is almost continuous, this behaviour is termed "continuous crack arrest". There is a sudden change in crack propagation rate as indicated by a kink on curve C; this is defined as "kink crack arrest".

Five types of failure mechanisms are relevant to the present composite systems, namely, fibre failure, fibre debonding, fibre pull-out, fibre bridging, and matrix failure. Usually, a single failure mechanism is not sufficient to explain the unique appearance of a fracture surface. The proportions of these mechanisms in the fracture process change with stress state and environment [5, 6]. For short-fibre composites, the fibre ends usually govern the failure mechanisms because the stress concentrations occur near fibre ends. Moreover, fibre ends retard corrosion effects along the fibre–matrix interface due to the lack of a continuous interfacial path [7]. The proposed models which represent the dominant failure mechamisms in the aligned short-fibre composites are: (a) fibre failure, (b) fibre pull-out,

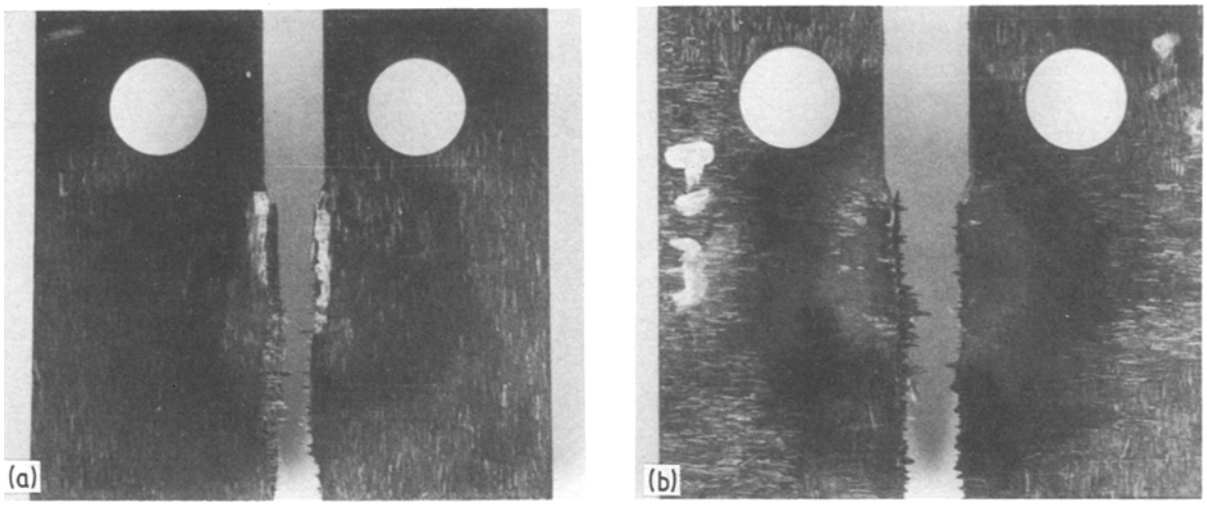

Figure 7 Failed specimens of short-hybrid composites tested in 1N H_2SO_4 (a) without pre-immersion, (b) with 60-day pre-immersion.

and (c) fibre–matrix interface debonding. These are discussed below.

The experimental results indicate that crack propagation behaviour of glass composites tested in 1 N H_2SO_4 obeys LEFM (Fig. 3). The crack growth curves are similar to curve A in Fig. 8; no crack arrest can be observed. Fig. 9 shows the characteristic feature of a large area of flat fracture normal to loading axis. Fibre failure dominates the cracking mechanism; a proposed microscopic failure model is illustrated in Fig. 10.

For hybrid composites tested in 1 N H_2SO_4 (Fig. 6), observation reveals that cracking follows a path which avoids carbon fibres and interacts mostly with glass fibres. This results in carbon fibre pull-out. The crack growth rate is then decreased but the change of growth rate is continuous. The crack growth behaviour is similar to that shown in Fig. 8, curve B (continuous crack arrest). Fig. 11 illustrates carbon fibre pull-out on the fracture surface of hybrid composites and Fig. 12 depicts the local cracking mechanism of this case.

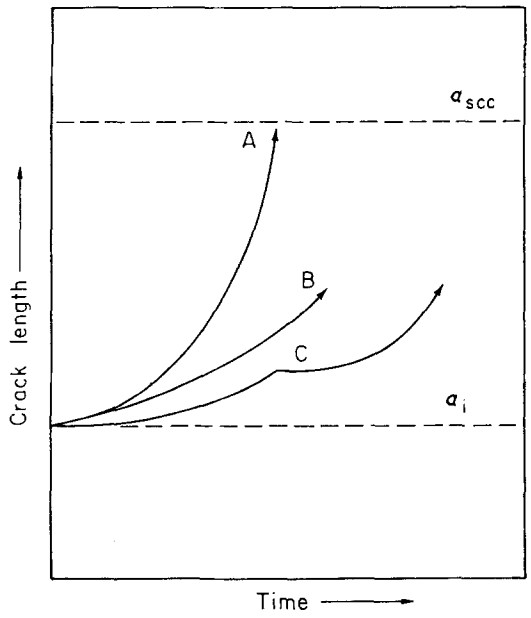

Figure 8 Crack length against time. A = LEFM; B = continuous crack arrest; C = kink crack arrest.

Fig. 13 depicts the local crack growth observed in glass and hybrid composites tested in air. After the initial crack growth, the crack propagates along the fibre–matrix interface in the transverse direction. This results in fibre bundle pull-out, a rugged appearance of the fracture surfaces and a sudden change of crack growth rate (kink crack arrest). Figs 14 and 15 show the pulled-out hybrid and glass fibre bundles, respectively.

4.2. K_I–t_f curve

The K_I–t_f curve is a very efficient tool for assessing the stress–corrosion effects on the useful life of a composite. The curve also provides information about K_{Iscc} and the failure time for a given stress intensity factor. For a compact tension specimen obeying LEFM, the Mode I stress intensity factor, K_I, can be presented in the form [8]:

$$K_I = \frac{P}{BW^{1/2}} f(a/W) \quad (2)$$

where P is the applied load, B is the specimen thickness, and $f(a/W) = f(\alpha) = (2 + \alpha)(0.886 + 4.64\alpha - 13.32\alpha^2 + 14.72\alpha^3 - 5.6\alpha^4)/(1 - \alpha)^{2/3}$ for $0.2 < a/W = \alpha < 0.8$. Substituting Equation 2 into Equation 1 and rearranging terms, Equation 1 becomes

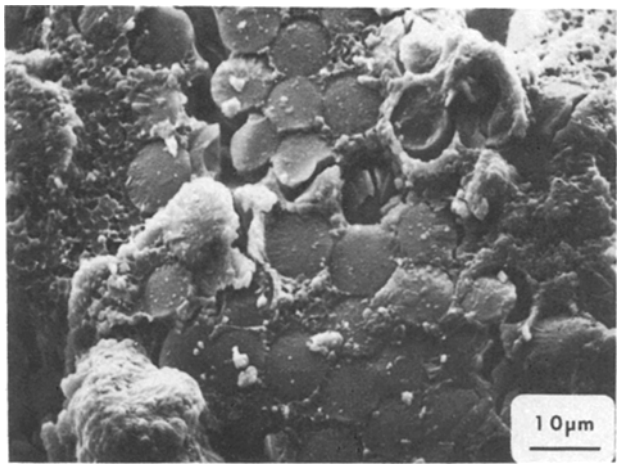

Figure 9 Flat fracture surface of short-glass composites tested in 1 N H_2SO_4.

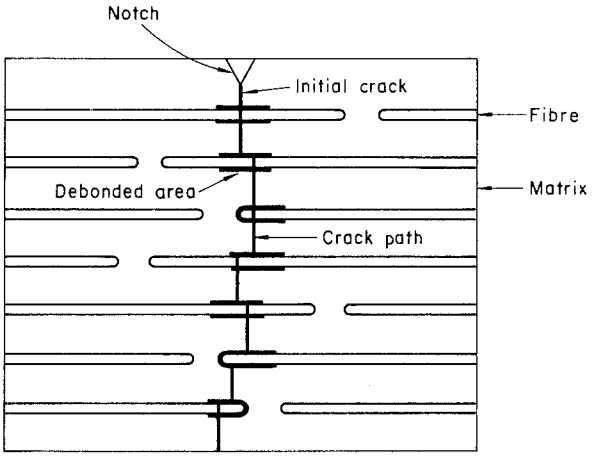

Figure 10 Fibre failure model.

$$\frac{W\,d\alpha}{C\left[\frac{P}{BW^{1/2}}f(\alpha)\right]^n} = dt \qquad (3)$$

Computations for the time to failure, t_f, can be performed by integrating Equation 3 with the starting and final normalized crack length, after the constant parameters have been determined from the experimental data. For example, if the data from glass specimen A in Fig. 4 are fitted with a polynomial of the form

$$\log V = \log C + n \log K_I \qquad (4)$$

then the values of log C and n can be obtained by a linear least squares method, where log C is the y-intercept and n is the slope of the calculated curve. The final results are $C = 3.4 \times 10^{-11}$ and $n = 6.34$ for $W = 0.051$ m, $P = 44.6$ kg $= 4.38 \times 10^{-4}$ MN ($K_I = 8.08$ MPa m$^{1/2}$) and $B = 0.0024$ m. Equation 3 then becomes

$$\frac{5.71 \times 10^9\,d\alpha}{[f(\alpha)]^{6.34}} = dt \qquad (5)$$

Using an experimentally determined time interval, 140 min, for the crack propagation between a normalized crack length (α/W) = 0.51 and final failure, and performing integration, Equation 5 can be expressed as

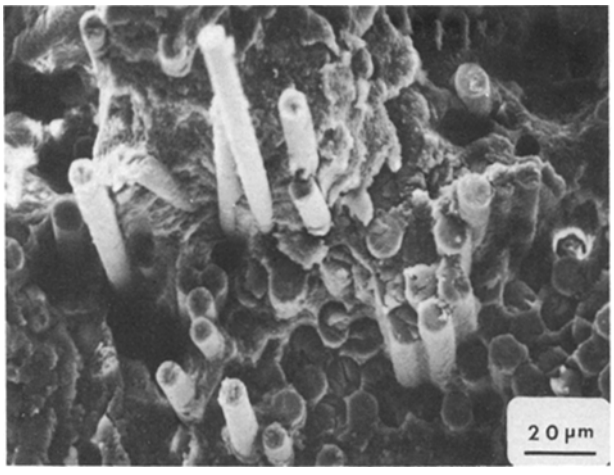

Figure 11 Carbon fibre pull-out on fracture surface of short-hybrid composites tested in 1 N H_2SO_4.

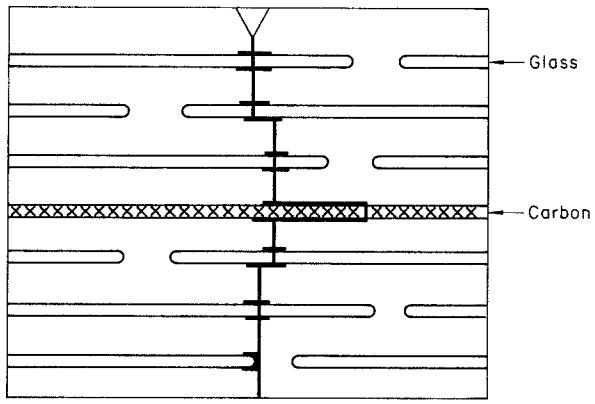

Figure 12 Fibre pull-out model.

$$t_f = \int_{\alpha_0}^{0.51} \frac{5.71 \times 10^9\,d\alpha}{[f(\alpha)]^{6.34}} + 140 \qquad (6)$$

where α_0 is the starting normalized crack length. To solve Equation 6, only the crack length, a, is needed, thus the k_I–t_f curve can be generated.

A comparison of calculated and experimental K_I–t_f curves of glass composite specimens is illustrated in Fig. 16; the calculated curve is in good agreement with experimental data. The three sets of experimental data exhibit very similar results indicating little or no effects of pre-immersion because glass fibres are well protected by the matrix. This is in agreement with the observations made by Friedrich [9] and Aveston and Sillwood [10]. The above results clearly indicate that the K_I–t_f curve of Fig. 16 is characteristic of LEFM behaviour of the material under stress-corrosion conditions.

Some other cases which cannot apply LEFM are given in Fig. 17; it is obvious that a corrosive environment does not affect cracking behaviour of short carbon composites, as discussed in Section 4.1. Fig. 18 illustrates the K_I–t_f curves for hybrid composites. All the curves do not follow LEFM predictions because crack arrests change the crack propagation behaviour.

5. Conclusions

Aligned short-fibre composites show very different characteristics from aligned continuous fibre

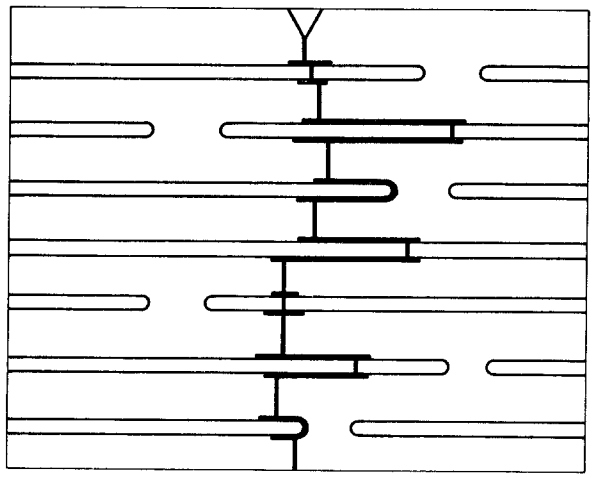

Figure 13 Fibre–matrix interface debonding model.

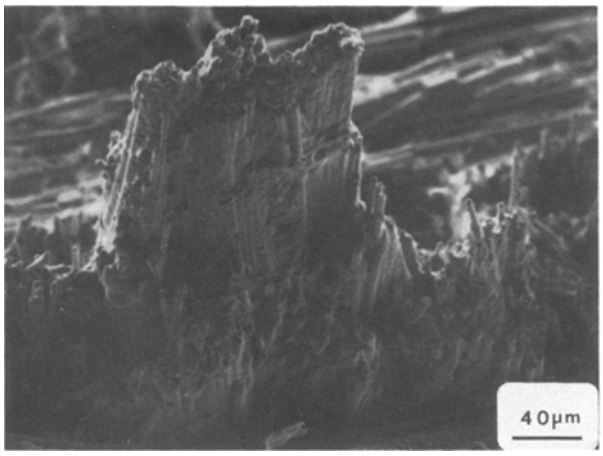

Figure 14 Fracture surface of short-hybrid composites tested in 1 N H_2SO_4.

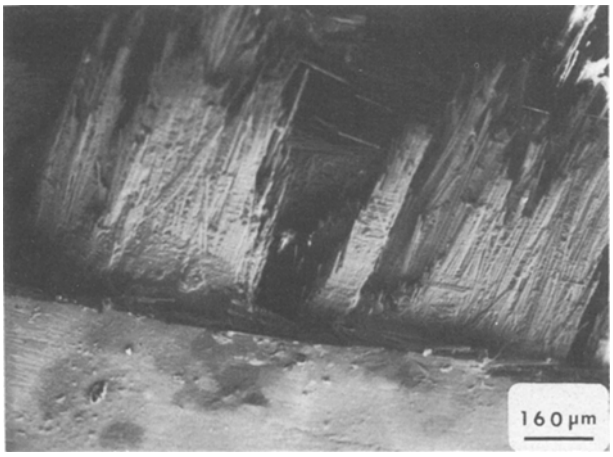

Figure 15 Fracture surface of short-glass composite tested in air.

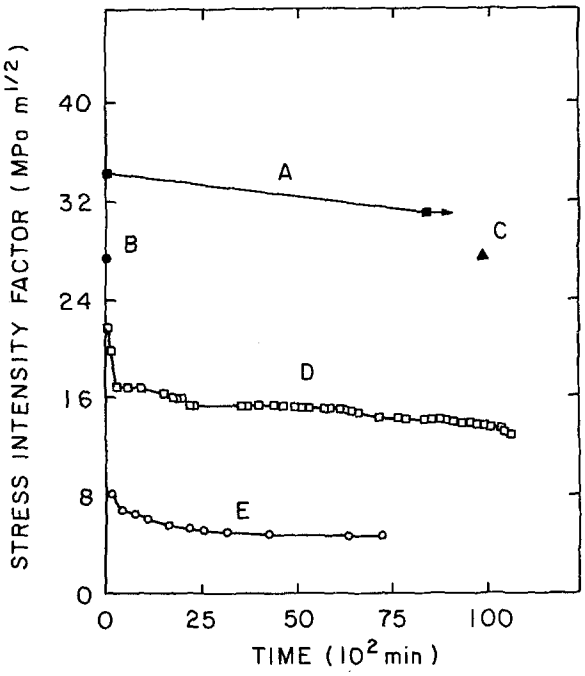

Figure 17 K_I–t_f curves of short-carbon composites tested in (A) air, (B) Instron machine, and (C) 1 N H_2SO_4; short-glass composites tested in (D) air and (E) 1 N H_2SO_4.

composites when they are tested in a corrosive environment. By studying the a–t and K_I–t_f curves, the degradation of crack resistance of composites due to stress-corrosion can be evaluated. Moreover, the K_I–t_f curves can be used to predict the service life of a composite containing cracks. The occurrence of crack arrests is determined by material properties, service environment, and pre-immersion conditions. The present research has quantified the susceptibility of aligned short glass, carbon and their hybrid reinforced epoxy composites to environmental attack.

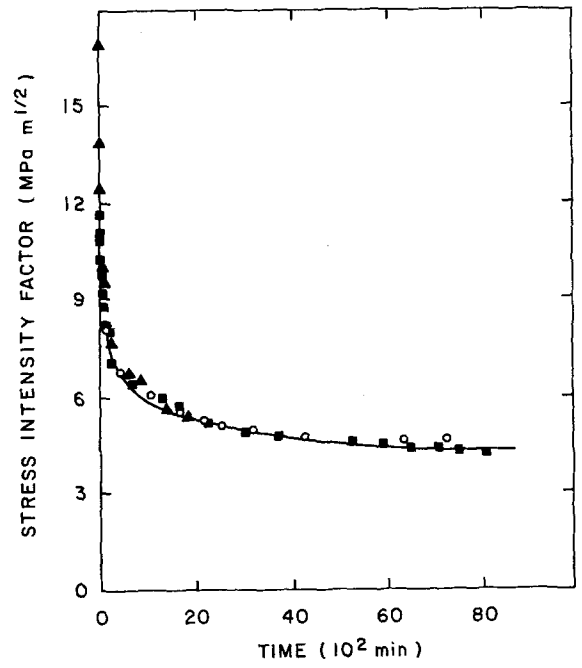

Figure 16 Theoretical and experimental K_I–t_f curves of short-glass composite tested in 1 N H_2SO_4. ——, Calculated curve. ○, without pre-immersion, K_{Ii} = 4.62 MPa m$^{1/2}$; ■, with pre-immersion, K_{Ii} = 4.13 MPa m$^{1/2}$; ▲, with pre-immersion, K_{Ij} = 5.45 MPa m$^{1/2}$.

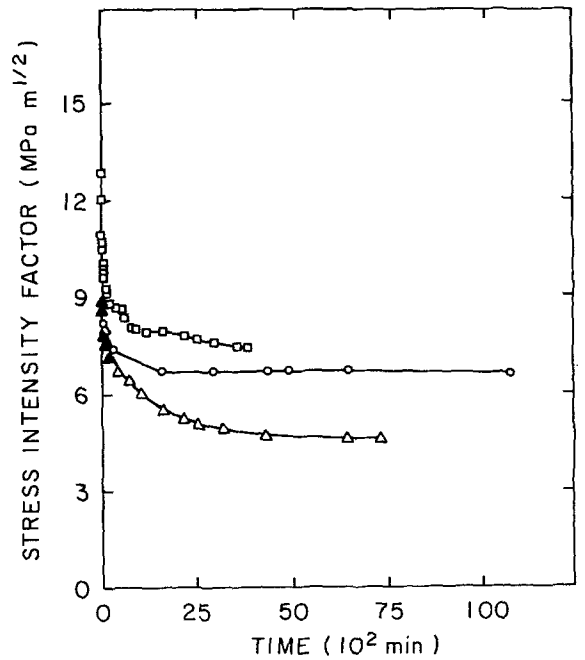

Figure 18 K_I–t_f curves of short-hybrid composites tested in 1 N H_2SO_4. Hybrid: ○, □, without pre-immersion; ▲, with pre-immersion. Glass: △, with and without pre-immersion.

Acknowledgement

This work was sponsored by the US Department of Energy under contract No. 03-7-21-3140-08.

References

1. H. EDWARDS and N. P. EVANS, in Proceedings of the Third International Conference on Composite Materials (ICCM), Paris (Pergamon, New York, 1980) p. 1620.
2. H. RICHTER, *ibid.* p. 387.
3. P. L. HSU and T. W. CHOU, in Proceedings of the Fifth ICCM, San Diego (The Metals Society, Warrendale, Pennsylvania, 1985) p. 1475.
4. P. W. MANDERS and T. W. CHOU, in Proceedings of the fourth ICCM, Tokyo (Japan Society for Composite Materials, 1982) p. 1075.
5. P. L. HSU, Msc thesis, University of Delaware (1984).
6. P. J. HOGG and D. HULL, in Proceedings of the Reinforced Plastic Congress, Brighton (The British Plastic Federation, London, 1982) p. 115.
7. R. F. REGESTER, *Corrosion* **25** (1968) 157.
8. J. E. SRAWLEY, *Int. J. Fracture* **12** (1976) 475.
9. K. FRIEDRICH, "Microstructure and Fracture of Fibre Reinforced Thermoplastic Polyethylene Terephthalate (Rynite)" Technical report no. 80-17. (Center for Composite Materials, University of Delaware, 1980).
10. J. A. AVESTON and J. M. SILLWOOD, *J. Mater. Sci.* **17** (1982) 3491.

Received 14 November 1985
and accepted 10 January 1986